Fast Detection of Open-Switch Fault in Cascaded H-Bridge Multilevel Converter

Mahmoud Shahbazi [a], MohammadReza Zolghadri [b*], Masih Khodabandeh [b], Saeed Ouni [b]
a. School of Engineering and Computing Sciences, Durham University, Durham, UK,
b. Center of Excellence in Power System Management & Control (CEPSMC), Sharif University of Technology, Tehran, Iran

***Abstract*—Cascaded H-Bridge converter has recently been utilized in different high-power applications due to its modular and simple structure. In order to have a balanced operation after a fault occurrence in this converter, it is necessary to detect the switch fault and its location. In this paper, a fast power switch fault detection method is presented to identify the fault and its location. Only one voltage measurement per phase is required by this method, and the fault detection is faster compared to the existing methods. Moreover, it is suitable for implementation on an FPGA device, due to the use of simple math, relational and state machine blocks. The proposed method is verified by computer simulations and FPGA-based experimental tests.**

***Keywords*—Power switch fault detection; open-switch fault; multilevel converter; cascaded H-bridge converter Insulated Gate Bipolar Transistor (IGBT).**

I. INTRODUCTION

Multilevel converters have been used in recent years in a large number of power electronics applications due to their benefits over the conventional two-level converters especially in high-power applications. Amongst structures for multilevel converters are diode clamped [1], flying capacitor [2] and Cascaded H-Bridge (CHB) converters [3-8]. CHB is consisted of cascaded connection of H-bridges in each phase, and therefore has been an interesting solution in high power applications due to its simple and modular structure. In this converter, each switching device has to withstand only a portion of the total voltage. Therefore, CHB can produce higher voltages, while producing lower harmonics.

However, having a large number of devices significantly increases the risk of a failure in one of the power converter switches. Therefore it is important to detect and compensate faults occurrence in these converters. Several methods are proposed for the post-fault operation of multilevel converter [9-17] providing the possibility of balanced operation of the converter even after a fault. The faster the fault is detected; the smaller will be its effect on the system performance. Also using a large number of additional sensors for Fault Detection (FD) will in turn increases the cost and reduces the system reliability; therefore it is desired to lower the number of additional sensors as much as possible.

In this paper, the cascaded H-bridge converter and open-circuit power switch fault detection are concerned. A diagram of a CHB converter is given in Fig. 1.

Few fault detection schemes are proposed in the literature for detection of the fault and its location in CHB converters. A method based on voltage magnitude measurement is presented in [18], but is relevantly slow in detecting faults. A fault can be detected within one fundamental cycle (a few milliseconds) in this method. In [12, 19], some methods based on the artificial intelligence are proposed for the fault detection in CHB. In [12] Neural Network (NN) classification is used for fault diagnosis. A multilayer perceptron network is used for detecting the type and location of the fault. Moreover, a genetic algorithm optimization technique is used to optimize the NN training. The fault detection time has been around six fundamental periods. Overall, this method is not very quick, is complicated for practical implementation, and also its performance depends on the correct training of the NN. A similar method is proposed in [19] which has the same drawbacks. In [20], the fault detection is based on the spectral analysis of the phase output voltage. The magnitude and phase angle of switching frequency component of the output phase voltage is observed in this method for fault detection. This method has better performance compared to previous ones, but it uses a complicated approach for fault detection that is not very easy to implement. Also this approach may experience difficulties in finding faulty cell's location when a higher number of cells is utilized. In [21], Fast Fourier Transform is used on the output voltages to preprocess these signals. Then PCA (Principal Component Analysis) is used to extract the fault signatures and finally multiclass Relevance Vector Machine (mRVM) is used to classify fault samples. Fault detection times of around 50-130 ms are reported in simulation and experimental test. However, the fault detection is very complicated, and still relatively slow.

In this paper, a very fast method for detection of open-switch

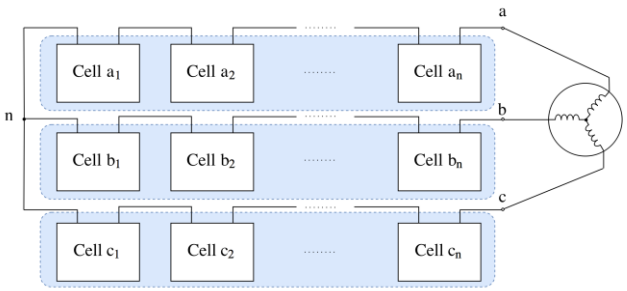

Fig. 1. Three-phase CHB.

faults is developed and then validated for multilevel CHB converters. This method is capable of detecting the fault and its location in a few hundreds of microseconds, which is several times faster compared to the previous methods [12, 19, 21] and is comparable with [20]. Moreover, the proposed method uses only simple math, relational and state machine blocks and therefore its implementation on a digital target like FPGA would be easy. Like previous methods, only the output phase voltage measurement is needed, therefore no additional cost is imposed on the system.

In the following, first the multilevel CHB converter is reviewed. Then, in section III, the proposed fault detection method is detailed. The simulation results are provided in section IV. The FD method is implemented on an FPGA, and experimental tests are carried out, and the results are discussed in section V. Both simulation and experimental tests are in accordance, and testify to the effectiveness and high performance of the proposed method.

II. MULTILEVEL CHB CONVERTER

A. The Structure

A three-phase CHB converter is shown in Fig. 1. Each cell is consisted of an H-bridge inverter and an isolated DC source. One cell is depicted in Fig. 2. Normally all DC sources have the same DC voltage. The switches' commands in each leg of the H-bridge inverter are complementary. An additional switch S_T is used between the two output terminals of the cell, allowing the cell to be bypassed, in case of a fault. In this way, other cells can continue powering the load [20].

Since each cell can produce three voltage levels, therefore the maximum voltage level of each output phase will be *2n+1*, where *n* is the number of the cells per phase.

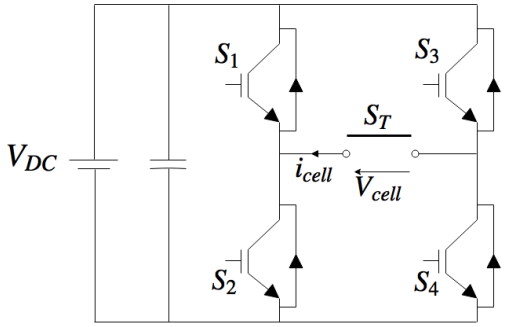

Fig. 2. One elementary cell of the CHB with bypass switch.

Different modulation methods are suggested for output voltage control of this topology. The most popular methods are Phase Shifted Pulse Width Modulation (PSPWM) and level-shifted PWM [21, 22]. PSPWM method is the most suitable PWM and is recommended for cascaded H-Bridge converters [23] and is extensively used for its ease of implementation and even power distribution amongst the cells. Moreover, this method produces "n" times lower switching losses than the level shifted PWM [23]. In this paper, the PSPWM is concerned, because of its better performances. In this method each cell is controlled as a unipolar PWM inverter. The same reference signal is used in all unipolar PWM blocks of a given phase while the carrier signals of the cells are shifted in respect to each other. In a CHB converter with "*n*" cells, the carrier signal of cell (*i*) is 180^o/n shifted in respect to the cell number (*i-1*). For each cell, the second carrier that is needed for its second leg (switches S3 and S4) is produced by negation of this carrier. Fig. 3 shows the operation principle for an 11-level (five cells per phase) converter. The effective output frequency is *2n* times the carrier frequency. Therefore even using a low switching frequency in each cell, it is possible to have an equivalent high switching frequency at the output of the converter. Hence the switching losses of each cell can be reduced. It is also evident that each switching has an effect on the output voltage, and as later is shown, it is possible to use this expected effect along with the measured output voltage to detect a fault.

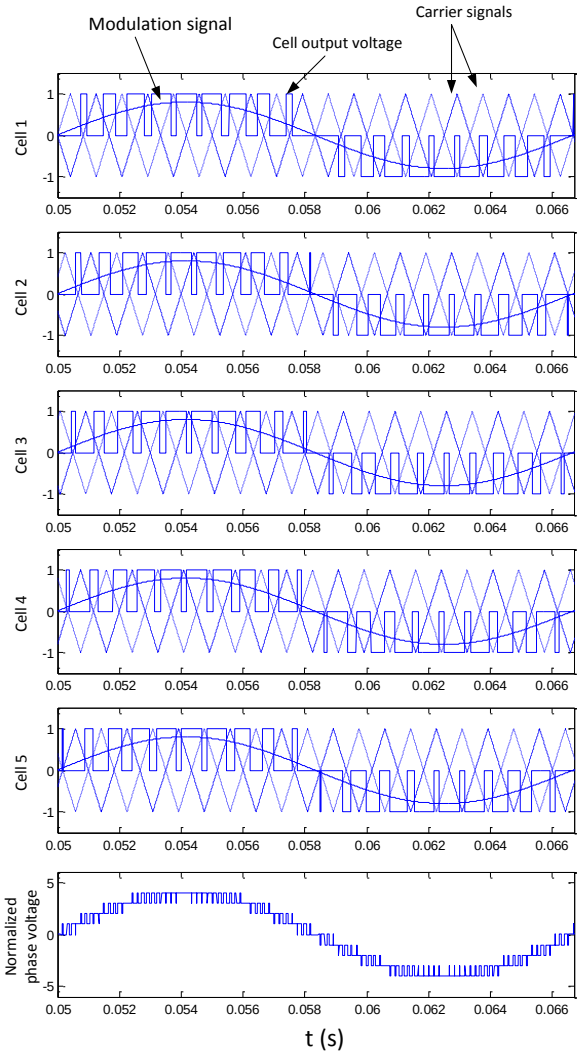

Fig. 3. Normalized values of the modulation and carrier signals, the cell output voltages and the phase output voltage in PSPWM for a five-cell (11-level) CHB converter.

III. FAULT DETECTION ALGORITHM

Fast fault detection is mandatory in power electronics converters in order to minimize the undesirable behavior of the

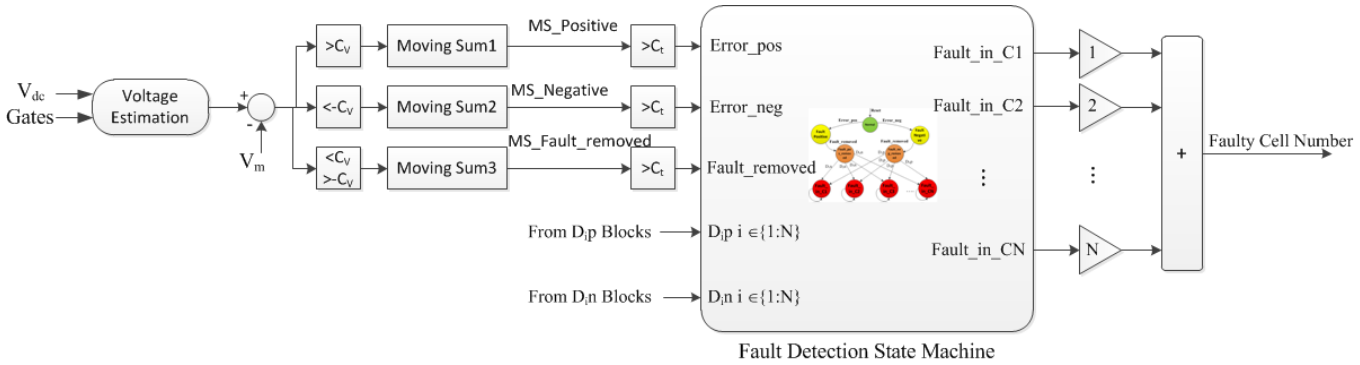

Fig. 4. Proposed fault detection scheme for CHB converter.

converter by changing the converter topology or the control method after fault detection. For DC-DC and conventional two-level converters, fast detection methods are proposed in [24, 25]. In this paper, a generalized version of those method is proposed for the CHB converter that not only detects the fault, but also can detect the faulty cell, which is necessary for the reconfiguration of the converter in order to be capable of using any of the post-fault control methods proposed in [12,16,18]. In this paper, open-circuit faults are considered. For short-circuit switch faults, normally using fast acting fuses the converter topology will become similar to that after an open-switch fault [24], or special supplementary hardware is needed to detect the fault, as the software methods are not fast enough to detect the short-circuit switch faults. It is also worth to mention that many drivers have the possibility to identify the short circuited switches and stop the operation [26, 27]. Nonetheless, this is not in the scope of this paper.

A. *Fault detection*

In ideal condition, an open switch fault can be easily detected by comparing the measured and estimated phase voltages of the converter. Considering a single cell (cell C) in one phase of a CHB converter as shown in Fig. 2, let us assume that the fault is in S_1 switch. Clearly, the observations can be generalized to other swithches as well. Gate command for switch k is shown with $T_k \in \{0,1\}$, and commands for two switches in each leg are complementary. The phase output current is shown by i_{cell} and V_{DC} is the DC voltage at the input of the cell (see Fig. 2). For a fault in S_1, when $T_1T_3 = 10$ and $i_{cell} < 0$, diode D_{S2} conducts instead of S_1, therefore while estimated output voltage is V_{DC} the measured voltage would be equal to 0. If $i_{cell} > 0$ however, diode D_{S1} conducts and the converter would behave normally, so no fault in the system can be detected. For the fault in S_1, estimated and measured voltages of the cell and the error between them are resumed in Table I. Here $V_{es,C}$ and $V_{m,C}$ represent the estimated and measured voltages of cell 'C', respectively. It is assumed that $i_{cell} < 0$, therefore the fault in S_1 will affect the output voltage of the cell.

Table I- ESTIMATED AND MEASURED VOLTAGES IN CASE OF AN OPEN SWITCH FAULT IN S_1 IN CELL C

T_1T_3	$V_{es,C}$	$V_{m,C}$	Error $V_{es,C} - V_{m,C}$
00	0	0	0
01	$-V_{DC}$	$-V_{DC}$	0
10	$+V_{DC}$	0	$+V_{DC}$
11	0	$-V_{DC}$	$+V_{DC}$

Since in other cells the measured and estimated voltages are equal in normal operation, the total error between measured and estimated voltages can be written as:

$$V_{es} - V_m = V_{es,C} - V_{m,C} = +V_{DC} \qquad (1)$$

Therefore the fault in any of the switches can be effectively detected.

However in practice, the estimated and measured voltages are always different, mostly due to measurement and discretizing errors, and more importantly because of non-ideal behaviors of the switches and the drivers, such as turn-off and turn-on delay times and dead time generated by the controllers or drivers. Therefore, to avoid false detection, separate time and voltage criteria must be adopted to account for the probable time and voltage mismatches. On the other hand, in order to make the fault tolerant control possible, not only the occurrence of a fault but also its location must be detected. Generally, it is necessary to detect the faulty cell, and bypass it to continue the operation of the converter. The proposed method is designed to account for voltage mismatches, and detect the fault and its location very quickly.

Fig.4 shows the proposed detection method. Only one voltage measurement per phase is required by this method, and it is consisted of simple blocks that make its implementation on FPGA easy. First the estimated voltage is produced using the gate commands of the switches and DC voltages of the cells. Then, error between estimated and measured voltages is calculated. Fault is detected by evaluating this error, using two levels of mismatch compensation for voltage and time, as discussed before. First, two comparators check if the voltage error amplitude is large enough. If the voltage error is larger than C_V or smaller than $-C_V$, output of these comparators become '1'. As it is previously seen, a fault will induce a

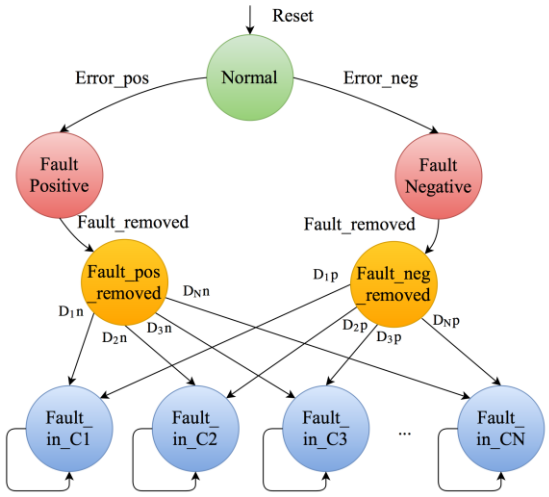

Fig. 5. Fault detection State machine.

voltage error equal to $\pm V_{DC}$, therefore choosing $C_V = V_{DC}/2$ seems very reasonable for voltage mismatch compensation.

Assuming that the fault detection algorithm operates with a 500 kHz clock, a moving sum is then performed for 15 sampling periods (equal to a window length of 30 μs) on these outputs to see on how many samples the voltage error has been considerable. Moving sum, also known as the running sum, is a simple form of a Finite Impulse Response (FIR) filter, and is defined as the sum of element over a moving window of values with length N, as shown in equation (2).

$$y(n) = x(n) + x(n-1) + \cdots + x(n-N+1) \qquad (2)$$

Here, the moving sum shows in how many of the last observed samples (the observation window), the input has been equal to one.

The outputs of the moving sum blocks then are investigated and if they are larger than C_t then one can be sure that a fault has occurred somewhere in the circuit. Since the observation window considers 15 samples, C_t is chosen equal to 12.

B. *Fault location identification*

After fault detection, it is necessary to detect the fault location as well. Here, a simple yet effective method is used based on the fact that when the command of the faulty switch goes back to zero, the voltage error will also disappear, because the converter will act normally again. The third comparison and moving sum unit detect the fault removal, and signal it to the fault detection state machine (FDSM). As it is visible in Fig. 4, when the error voltage is less than C_V and larger than $-C_V$ for at least C_t samples, one can be sure that there is no fault in the system, and the *Fault_removed* input of the FDSM will become equal to 1. The FDSM is shown in Fig. 5.

If a fault is already detected, one of the *Fault_positive* or *Fault_negative* states in FDSM are active, and the SM is waiting for the Fault removal signal (*Fault_removed*) to arrive. When this signal arrives, it is only necessary to investigate in which cell(s) a switching is occurred in the previous C_t samples. This is done with the help of $D_i p$ and $D_i n$ signals. Fig. 6 shows the $D_i p$ and $D_i n$ generation for one cell. For each cell,

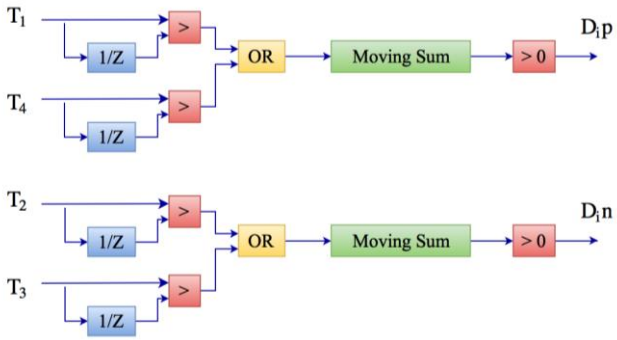

Fig. 6. generation of $D_i p$ and $D_i n$ signals.

these signals basically show if in the last C_t sampling a switching is commanded that increase or decrease the cell's output voltage. In other words, $D_i p$ means that a positive voltage step is commanded, and $D_i n$ means that a negative voltage step is commanded.

Basically a switching in S_1 or S_4 will tend to increase the output voltage by V_{DC} while a switching in S_2 or S_3 will decrease it by V_{DC}. That is why in Fig. 6, T_1 and T_4 are associated with $D_i p$ (positive voltage step) while T_2 and T_3 are associated with $D_i n$ (negative voltage step). If the error has been positive and the fault removal signal arrives, it can be concluded that a decreasing switching has been occurred, which corresponds to one $D_i n$ signal going high. Based on the $D_i n$ signals, the next state in the FDSM can be detected. For a negative error similar reasoning applies. The FDSM stays in the faulty states ($Fault\_in\_Ci$, $i \in \{1{:}N\}$) upon entering them, as long as a reset signal is not applied.

Finally, the $Fault\_in\_Ci$ outputs go high when the corresponding state is active. These outputs may be used in the fault tolerant scheme, to reconfigure the structure and control appropriately. In Fig. 4, their information is combined to determine the faulty cell's number.

It is worth mentioning that after reconfiguration, the FDSM can be reset, and fault detection will be again possible for other switches, as long as the necessary changes in the calculation of the estimated voltage are applied.

One special condition is particularly interesting, when two switchings have occurred in two legs during the last C_t sampling periods, because it is important to detect which one has been responsible for fault removal. In another words, it is

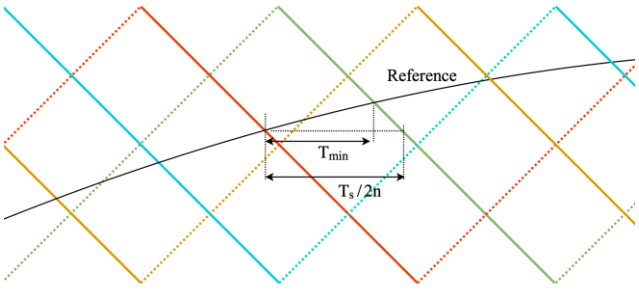

Fig. 7. Minimum time between two consecutive rising levels.

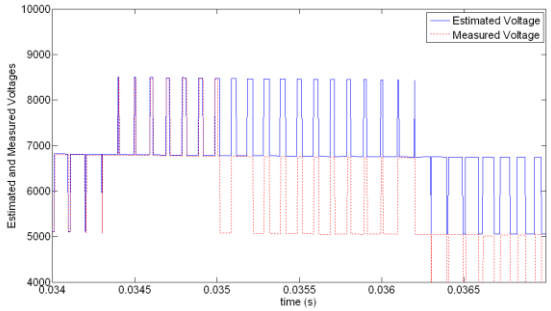

Fig. 8. Estimated and measured phase voltages for a fault at t=0.035s.

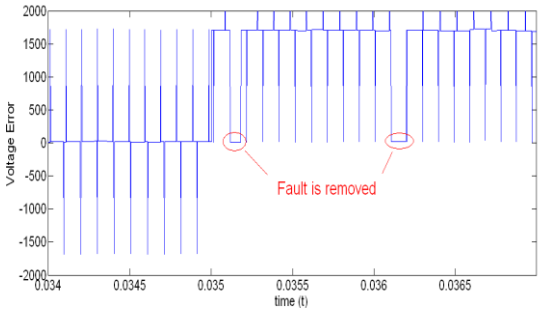

Fig. 9. Voltage error between estimated and measured phase voltages for a fault at t=0.035s.

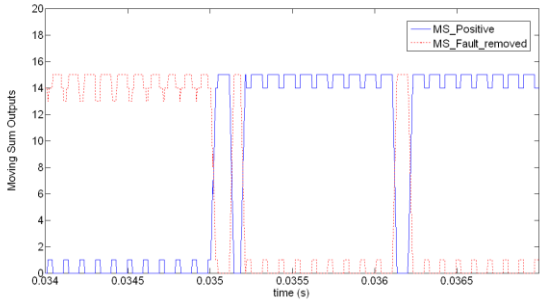

Fig. 10. Output of the moving Sum 1 and 3 for a fault at t=0.035s.

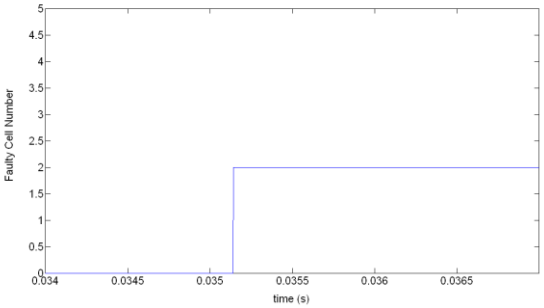

Fig. 11. Detection of the fault and its location for a fault at t=0.035s.

important that in the observation window, only one $D_i p$ and $D_i n$ are present, otherwise the FDST cannot decide between two $D_i p$ or $D_i n$ signals. Fig. 7 shows an example of such condition for a Phase Shifted PWM (PSPWM). Referring to Fig. 3, it can be verified that when a carrier becomes larger than the modulation signal, voltage of the corresponding cell will experience a $+V_{DC}$ change (rising level) and vice versa. The modulation signal frequency is several times smaller than the carrier frequency, therefore it can be visually confirmed in Fig. 7 that the minimum time between two $+V_{DC}$ or two $-V_{DC}$transitions it equal to

$$T_{min} \cong \frac{1}{2Nf_s} \tag{3}$$

If this minimum time is larger than the sampling window, the fault detection algorithm sees only one positive or negative transition, and therefore it can detect the fault effectively. Normally, this minimum time is at least several times larger than the length of sampling window. Here, a conservatively large window time of $T_{window} = 30\mu s$ is used, in accordance with the value for experimental setups reported in [25], therefore if $T_{min} > 30\mu s$ the FDA can work correctly. For a 5-cell converter, this translates to switching frequency calculated as below:

$$f_s < \frac{1}{2*5*30\mu s} = 3333\ Hz \tag{4}$$

Normally the switching frequency is well beyond this limit, even with the conservative choice of T_{window} in this study.

IV. Simulation Results

Simulations are carried out to evaluate the effectiveness of the proposed method. A five-cell (11-level) three-phase CHB converter is simulated. DC-link voltages of the cells are equal to 1700 V. The fundamental switching frequency is equal to 1000 Hz, resulting in a $2 * n * f = 2 * 5 * 1000 = 10\ (kHz)$ equivalent switching frequency. We consider an open-loop control of the converter and using PSPWM, it generates a sinusoidal voltage at the converter's output. A fault is introduced in switch S_1 of cell 2 at *t=0.035s*. The fault detection algorithm operates with a 500 kHz clock. As soon as the estimated and measured voltages are different, based on the sign of the voltage error, the *MS_positive* or *MS_negative* (ref. Fig. 4) signals will start to increase, and when one of them becomes greater than 12, the fault is detected and one of the

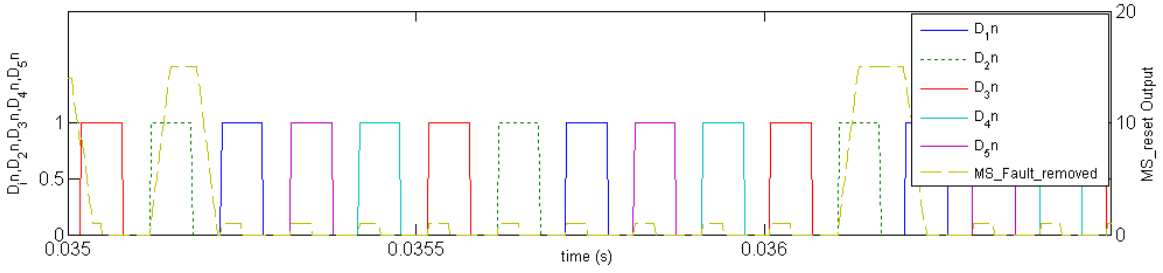

Fig. 12. Detection of fault location.

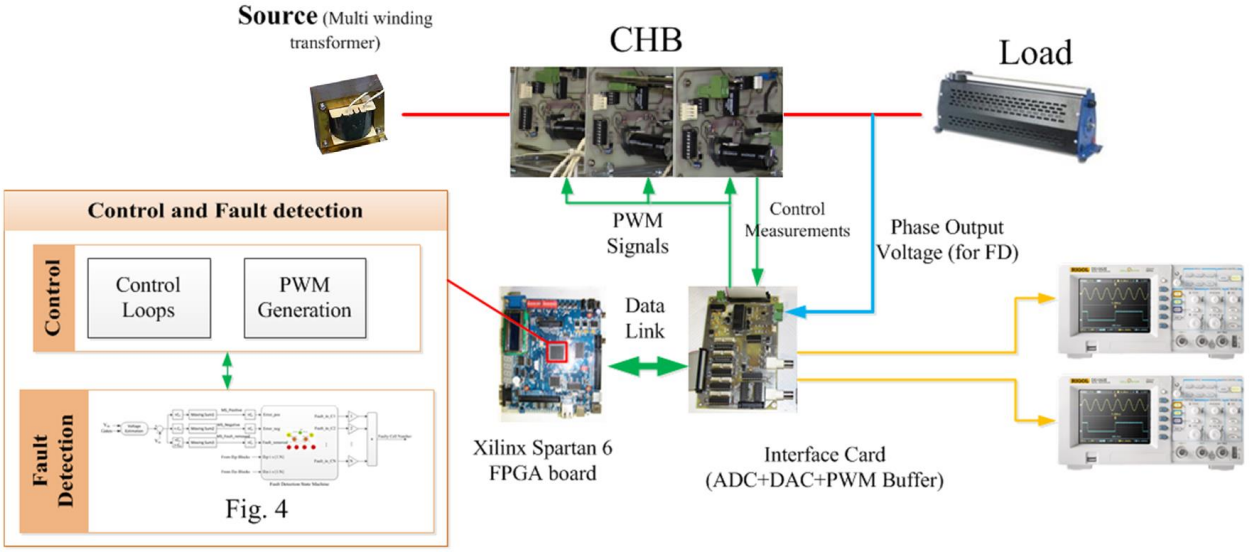

Fig. 13- the experimental setup

Fault_positive or *Fault_negative* states will become active.

Here, the estimated and measured voltages of the faulty phase are shown in Fig. 8. The voltage error is shown in Fig. 9. As it was expected, a fault in S_1 has resulted in a $+V_{DC}$ error in phase voltage. It is also shown in this figure that in certain periods of time, the voltage error disappears. This is due to a decreasing switching command, and is used for identification of the fault's location.

Outputs of the Moving Sum 1 and Moving Sum 3 blocks are shown in Fig. 10. *MS_Positive* signal starts to increase when a large enough positive voltage error exists. When it passes $C_t = 12$, a fault can be declared, and the FDSM goes to the *Fault positive* state. *MS_Fault_removed* signal starts to increase when the converter is acting normal or when the voltage error is smaller than its limits. It can be seen that during normal operation of the converter, this signal has a usually high value, but immediately after the fault occurrence at *t=0.035*, it goes down to zero. However, when the fault is removed due to switching in the faulty cell, this signal goes high again.

Fig. 11 shows the moment that the FDSM has reached its final stage, as well as the final result. Fault location is correctly detected. Also the fault detection has been very fast. The fault is detected in less than $200\mu s$.

Fig. 12 shows the details of the identification of fault location. The *MS_Fault_removed* signal is repeated here and shown with dashed line. When this signal goes higher than 12, the FDSM will enter the *Fault_positive_removed* state, and after that will choose its next state based on the $D_i n$ signals. It is shown in Fig. 12 that $D_2 n$ is high, meaning that the fault is disappeared as a result of switching in cell 2. Therefore, the next and last state in FDSM will be Fault_in_C2, and the faulty cell number will be equal to 2.

it is worth mentioning that since fault detection uses the switching information of the faulty cell, in the worst case the fault detection may take up to one switching period. On the other hand the minimum detection time happens when a fault is followed by *Error_pos* or *Error_neg* signals and then consequently followed by *Fault_removed* signal, without any delays in between. In this case, the fault detection will take $2C_t$ samples, which is equal to $48\mu s$ here. Also fault detection has an inherent robustness, as a result of the windowing technic that makes it possible to observe a signal for a long enough time before making any decision. The detection time is several times smaller than the values reported in [12, 18, 19], and is comparable to the result of [20]. However this method is simpler than the method proposed in [20] which needs complicated frequency spectrum analysis. Also due to the use of simple math, comparison and state machine blocks it is better suited for implementation on an FPGA.

V. Experimental Results

In order to verify the effectiveness of the proposed scheme further, an experimental setup is built in our laboratory. Fig. 13 shows the structure of this setup. A seven-level CHB is implemented by cascading three cells in each phase. For switches, IRF540 MOSFETs are used and HIP4082 bridge drivers are used for gating them. The control and fault detection schemes are implemented on a XC6SLX9 Spartan 6 FPGA from Xilinx, which has over 9k logic cells. An interface board is built as well with ADC, DAC and PWM buffer functions. AD7829 is used for analog to digital conversion, with 500 kSPS conversion rate on each of its 4 used channels. AD7302 two-channel DAC with 8-bit resolution and maximum 2us settling time is used for visualization of the digital fault detection signals. The control and detection use a clock of 500 kHz. All the delays on the control and detection loop, (including the A/D conversion, switch on and off time and deadtime, driver and optocoupler delay) are estimated to be less than 10 us, and therefore a conservative observation window for FD is chosen equal to 30us. Waveforms are captured using two two-channel oscilloscopes that are externally triggered by the fault occurrence signal.

A fault is applied to S_1 in $Cell1$ via a push button on the FPGA board. Fault is produced by setting the gate command of the faulty switch to zero. Fig. 14 shows the fault detection signals. The outputs of MS1 (*MS_Positive*) and MS3 (*MS_fault_removed*) are shown in this figure. These two signals are visualized using the two DAC outputs on the interface board. Since a fault in S_1 will result in a positive voltage error, only the output of the positive moving sum (*MS_Positive*) is shown and *MS_negative* does not include useful information, and therefore is not observed.

Before fault occurrence, the *MS_Positive* has limited output value. Small fluctuations in *MS_Positive* before fault occurrence are mostly due to the delays and deadtime in the system. However, it can be verified that when the fault is applied, there will be a positive voltage error for a considerable amount of time, and hence the *MS_Positive* will start to increase to higher values. The *MS_fault_removed* output will decrease accordingly.

Fig. 15 shows the details of fault occurrence and fault detection moments, as well as the switching command of the faulty switch. These waveforms are also captured upon fault occurrence, and hence have the same timing characteristics of those of Fig. 14. Fault occurrence and fault detection are merged into one signal and shown in this figure as *Fault-Fault_in_C1*, to empty the second axis for the switching signals of the faulty switch. From these two figure it is obvious that when the switching signals of the faulty switch has returned to zero, the converter is acting normally again. Therefore as it can be seen in Fig. 14 the *MS_fault_removed* output will increase and the *MS_Positive* output will decrease. Once the *MS_fault_removed* reaches its threshold, the FDSM of Fig. 4 will detect the faulty cell. The difference between *Fault* and *Fault_in_C1* is reduced to zero after this point, which attests that the fault and its location are correctly detected. The fault detection in this particular example has been around 350 us. Obviously, fault is detected 30 us after the first turn-off command of the faulty switch, therefore as it was previously mentioned, fault detection can be as fast as 2*observation window (60 us in this case), and in the worst case, it can take up to one switching period. Therefore, while the clock rate of FPGA and possibly the sampling rate of the ADC can be higher, higher values do not increase the fault detection speed further and hence are not necessary.

Table II summarizes the fault detection time in this paper with the other methods available in the literature.

Overall, the experimental results are in accordance with the simulation results and show the effectiveness of the proposed method for fast fault detection in CHBs. The output of this fault detection method can be used in order to make a fault-tolerant system that is able to use the information of fault and its location to reconfigure the system and its control, in order to make the continuity of service possible.

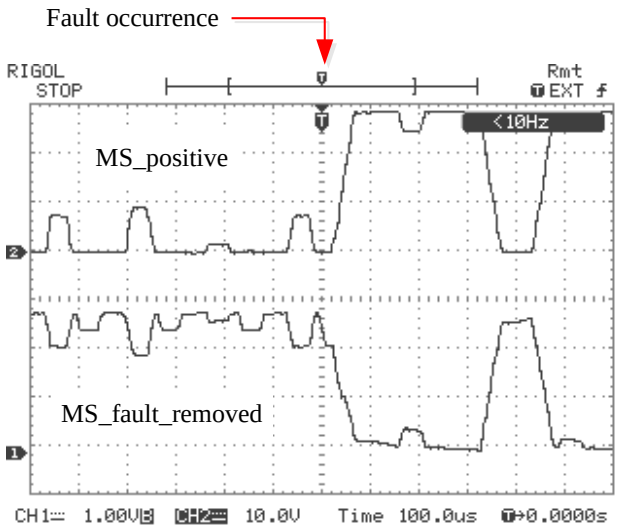

Fig. 14- Inputs to FDSM, from top to bottom: *MS_positive* and *MS_fault_removed*.

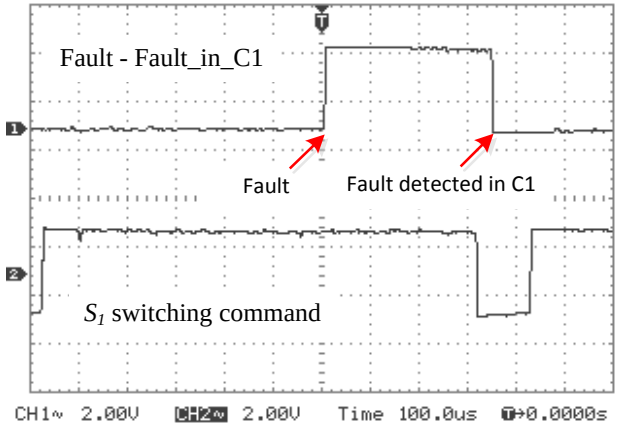

Fig. 15- Fault detection signals, from top to bottom: *Fault-Fault_in_C1*, S_1 switching command.

VI. Conclusion

In this paper, a very fast method for detection of open-switch faults in cascaded H-bridge converters is proposed. This method only needs one voltage measurement per phase, and is fast and robust for the detection of semiconductor open-switch fault and its location. The proposed method detects the fault by comparing the estimated and measured phase voltages of the converter. Fault location is found based on the fact that when

Table II- Comparison of fault detection time of different methods

Method	Complexity	Fault detection time
AI-based [12, 19]	Complex (NN training)	6 fundamental cycles
Method of [18]	simple	About 1 fundamental cycle
Voltage frequency analysis [20]	Complex (frequency analysis)	$\leq T_s$ (1 switching cycle)
PCA + mRVM [21]	Complex	50-130 ms
Proposed method	simple	$\leq T_s$ (1 switching cycle)

the faulty switch command is equal to zero, converter will act normal again. Only simple math, relational and state machine blocks are used and therefore the implementation of this approach on a digital target like FPGA will be easy. The detection time will be at maximum equal to one switching period and can be as low as a few tens of microseconds. Simulations and also experimental results are carried out, and their results show the high performance of the proposed method. Fault is detected in $350\mu s$. The output of this detection method can be used in fault-tolerant control schemes to make the continuity of service of the converter after a fault occurrence possible.

REFERENCES

[1] J. Pou, J. Zaragoza, S. Ceballos, M. Saeedifard and D. Boroyevich, "A carrier-based PWM strategy with zero-sequence voltage injection for a three-level neutral-point-clamped converter," *Power Electronics, IEEE Transactions on,* vol. 27, no. 2, pp. 642-651, 2012.

[2] B. P. McGrath and D. G. Holmes, "Enhanced voltage balancing of a flying capacitor multilevel converter using phase disposition (PD) modulation," *Power Electronics, IEEE Transactions on,* vol. 26, no. 7, pp. 1933-1942, 2011.

[3] J. A. Barrena, L. Marroyo, M. Á. R. Vidal, and J. R. T. Apraiz, "Individual voltage balancing strategy for PWM cascaded H-bridge converter-based STATCOM," *Industrial Electronics, IEEE Transactions on,* vol. 55, pp. 21-29, 2008.

[4] E. Villanueva, P. Correa, J. Rodriguez, and M. Pacas, "Control of a single-phase cascaded H-bridge multilevel inverter for grid-connected photovoltaic systems," *Industrial Electronics, IEEE Transactions on,* vol. 56, pp. 4399-4406, 2009.

[5] T. Zhao, G. Wang, S. Bhattacharya and A. Q. Huang, "Voltage and power balance control for a cascaded H-bridge converter-based solid-state transformer," *Power Electronics, IEEE Transactions on,* vol. 28, no. 4, pp. 1523-1532, 2013.

[6] S. Vazquez, J. I. Leon, J. M. Carrasco, L. G. Franquelo, E. Galvan, M. Reyes, J. A. Sanchez and E. Dominguez, "Analysis of the power balance in the cells of a multilevel cascaded H-bridge converter," *Industrial Electronics, IEEE Transactions on,* vol. 57, no. 7, pp. 2287-2296, 2010.

[7] K. Prasad, G. R. Kumar, T. V. Kiran and G. Narayana, "Comparison of different topologies of cascaded H-Bridge multilevel inverter," in *Computer Communication and Informatics (ICCCI), 2013 International Conference on*, 2013.

[8] B. P. McGrath, D. G. Holmes and W. Y. Kong, "A decentralized controller architecture for a cascaded H-bridge multilevel converter," *Industrial Electronics, IEEE Transactions on,* vol. 61, no. 3, pp. 1169-1178, 2014.

[9] P. Barriuso, J. Dixon, P. Flores, and L. Morán, "Fault-tolerant reconfiguration system for asymmetric multilevel converters using bidirectional power switches," *Industrial Electronics, IEEE Transactions on,* vol. 56, pp. 1300-1306, 2009.

[10] Aleenejad, Mohsen, et al. "A New Fault-Tolerant Strategy Based on a Modified Selective Harmonic Technique for Three-Phase Multilevel Converters With a Single Faulty Cell." *Power Electronics, IEEE Transactions on,* vol. 31, no. 4, pp. 3141-3150, 2016.

[11] S. Ouni, N. Noroozi, M. Shahbazi, M.R. Zolghadri, and H. Oraee; "A new fault tolerant scheme for cascaded H-Bridge multilevel converter." In Electric Power and Energy Conversion Systems (EPECS), 2013 3rd International Conference on, pp. 1-5. IEEE, 2013.

[12] S. Khomfoi and L. M. Tolbert, "Fault diagnosis and reconfiguration for multilevel inverter drive using AI-based techniques," *Industrial Electronics, IEEE Transactions on,* vol. 54, pp. 2954-2968, 2007.

[13] Ghazanfari, Amin, and Yasser Abdel-Rady I. Mohamed. "A Resilient Framework for Fault-Tolerant Operation of Modular Multilevel Converters." IEEE Transactions on Industrial Electronics, vol. 63, no.5, pp. 2669-2678, 2016.

[14] Li, Binbin, et al. "Fault Diagnosis and Tolerant Control of Single IGBT Open-Circuit Failure in Modular Multilevel Converters." IEEE Transactions on Power Electronics vol. 31, no. 4, pp. 3165-3176, 2016.

[15] G. P. Adam, K. H. Ahmed, S. J. Finney, K. Bell and B. W. Williams, "New breed of network fault-tolerant voltage-source-converter HVDC transmission system," *Power Systems, IEEE Transactions on,* vol. 28, no. 1, pp. 335-346, 2013.

[16] P. Correa, M. Pacas and J. Rodriguez, "Modulation strategies for fault-tolerant operation of H-bridge multilevel inverters," in *Industrial Electronics, 2006 IEEE International Symposium on*, 2006.

[17] M. A. Parker, C. Ng and L. Ran, "Fault-tolerant control for a modular generator converter scheme for direct-drive wind turbines," *Industrial Electronics, IEEE Transactions on,* vol. 58, no. 1, pp. 305-315, 2011.

[18] Yazdani, H. Sepahvand, M. L. Crow and M. Ferdowsi, "Fault detection and mitigation in multilevel converter STATCOMs," *Industrial Electronics, IEEE Transactions on,* vol. 58, no. 4, pp. 1307-1315, 2011.

[19] S. Khomfoi and L. M. Tolbert, "Fault diagnostic system for a multilevel inverter using a neural network," *Power Electronics, IEEE Transactions on,* vol. 22, pp. 1062-1069, 2007.

[20] P. Lezana, R. Aguilera, and J. Rodríguez, "Fault detection on multicell converter based on output voltage frequency analysis," *Industrial Electronics, IEEE Transactions on,* vol. 56, pp. 2275-2283, 2009.

[21] Wang, Tianzhen, et al. "Cascaded H-Bridge Multilevel Inverter System Fault Diagnosis Using a PCA and Multiclass Relevance Vector Machine Approach." *Power Electronics, IEEE Transactions on,* vol. 30 no. 12, pp. 7006-7018, 2015.

[22] R. Naderi and A. Rahmati, "Phase-shifted carrier PWM technique for general cascaded inverters," *Power Electronics, IEEE Transactions on,* vol. 23, pp. 1257-1269, 2008.

[23] S. Kouro, P. Lezana, M. Angulo, and J. Rodriguez, "Multicarrier PWM with DC-link ripple feedforward compensation for multilevel inverters," *Power Electronics, IEEE Transactions on,* vol. 23, pp. 52-59, 2008.

[24] M. Malinowski, K. Gopakumar, J. Rodriguez, and M. A. Perez, "A survey on cascaded multilevel inverters," *Industrial Electronics, IEEE Transactions on,* vol. 57, pp. 2197-2206, 2010.

[25] M. Shahbazi, M. R. Zolghadri, P. Poure, S. Saadate, "Fast detection of open-switch faults with reduced sensor count for a fault-tolerant three-phase converter", Power Electronics, Drive Systems and Technologies Conference (PEDSTC), pp. 546-550, 2011.

[26] M. Shahbazi, E. Jamshidpour, P. Poure, S. Saadate, M. R. Zolghadri, "Open and Short-Circuit Switch Fault Diagnosis for Non-Isolated DC-DC Converters Using Field Programmable Gate Array", IEEE Trans. on Industrial Electronics, vol. 60, no. 9, pp. 4136-4146, Sep. 2013.

[27] MC33153 Single IGBT Gate Driver, Semiconductor Components Industries, LLC, 2013, August, 2013 − Rev. 8.

[28] Smart Gate Driver Coupler TLP5214, Toshiba Corporation. Rev.1.0 Aug/12/2014.